THE JOURNAL OF BIOLOGICAL CHEMISTRY VOL. 287, NO. 45, pp. 37611–37620, November 2, 2012

Allosteric Communication between the Pyridoxal 5′-Phosphate (PLP) and Heme Sites in the H_2S Generator Human Cystathionine β-Synthase*

Received for publication, August 29, 2012, and in revised form, September 11, 2012 Published, JBC Papers in Press, September 13, 2012, DOI 10.1074/jbc.M112.414706

Pramod Kumar Yadav, Peter Xie, and Ruma Banerjee[1]

From the Department of Biological Chemistry, University of Michigan Medical Center, Ann Arbor, Michigan 48109-0600

Background: Long range allosteric communication between the heme and PLP cofactors occurs in human cystathionine β-synthase.
Results: Seven mutations in the PLP pocket were studied, including one described in homocystinuric patients.
Conclusion: The mutations perturb the heme electronic environment 20 Å away and increase propensity for forming an inactive species.
Significance: Bidirectional communication between heme and PLP occurs via an α-helix; its disruption is associated with disease.

Human cystathionine β-synthase (CBS) is a unique pyridoxal 5′-phosphate (PLP)-dependent enzyme that has a regulatory heme cofactor. Previous studies have demonstrated the importance of Arg-266, a residue at the heme pocket end of α-helix 8, for communication between the heme and PLP sites. In this study, we have examined the role of the conserved Thr-257 and Thr-260 residues, located at the other end of α-helix 8 on the heme electronic environment and on activity. The mutations at the two positions destabilize PLP binding, leading to lower PLP content and ~2- to ~500-fold lower activity compared with the wild-type enzyme. Activity is unresponsive to PLP supplementation, consistent with the pyridoxine-nonresponsive phenotype of the T257M mutation in a homocystinuric patient. The H_2S-producing activities, also impacted by the mutations, show a different pattern of inhibition compared with the canonical transsulfuration reaction. Interestingly, the mutants exhibit contrasting sensitivities to the allosteric effector, *S*-adenosylmethionine (AdoMet); whereas T257M and T257I are inhibited, the other mutants are hyperactivated by AdoMet. All mutants showed an increased propensity of the ferrous heme to form an inactive species with a 424 nm Soret peak and exhibited significantly reduced enzyme activity in the ferrous and ferrous-CO states. Our results provide the first evidence for bidirectional transmission of information between the cofactor binding sites, suggest the additional involvement of this region in allosteric communication with the regulatory AdoMet-binding domain, and reveal the potential for independent modulation of the canonical transsulfuration *versus* H_2S-generating reactions catalyzed by CBS.

Cystathionine β-synthase (CBS)[2] is a pyridoxal 5′-phosphate (PLP)-dependent enzyme that catalyzes the condensation of serine and homocysteine to give cystathionine and water, the first step in the transsulfuration pathway (1–3). Alternatively, CBS can generate cystathionine by condensation of cysteine and homocysteine or form lanthionine by condensation of 2 mol of cysteine (4). The latter two reactions lead to elimination of H_2S. Mutations in the CBS gene are inherited in an autosomal recessive manner and lead to homocystinuria, which is associated with multiple clinical pathologies, including cardiovascular disease, skeletal deformities, and lens dislocation (5). Human CBS is a dimeric protein with a tendency to aggregate to higher oligomeric forms (6). Each subunit comprises three domains: an N-terminal heme-binding domain, a central PLP-binding catalytic domain, and a C-terminal regulatory domain, which binds the allosteric activator, *S*-adenosylmethionine (AdoMet) (7). The presence of heme in CBS from higher but not lower eukaryotes is enigmatic, and in fact, CBS is the only known PLP-containing hemeprotein (8, 9).

Each subunit of CBS binds a single heme and PLP that are separated by ~20 Å (10–12). In human CBS, the axial ligands to the heme are Cys-52 and His-65, and the heme is low spin and hexacoordinate in both the ferrous and ferric states (13, 14). The distance from the active site clearly precludes a direct role for the heme in the catalytic cycle. Instead, multiple studies point to a regulatory role for this cofactor, which upon binding of gaseous molecules, such as NO or CO, inhibits CBS activity (15–18). Binding of CO to ferrous CBS displaces the Cys-52 ligand (19), whereas the ferrous-NO heme is pentacoordinate, indicating loss of both endogenous ligands (16). The two hemes in CBS exhibit unequal affinity for CO, with K_d values of 1.5 ± 0.1 and 68 ± 14 μM, respectively (15, 16). NO binds 200-fold less tightly than CO and exhibits a K_d of 281 ± 50 μM (16). Recently, we demonstrated inhibition of CBS by reductive carbonylation in the presence of NADPH and a cytoplasmic flavoprotein, methionine synthase reductase (18). This inhibition was reversed by air oxidation or photolysis of the ferrous-CO adduct.

The considerable distance between the heme and PLP sites begs the question as to how changes in the heme environment are transduced to the active site and, in turn, lead to enzyme

* This work was supported, in whole or in part, by National Institutes of Health Grant HL58984.
[1] To whom correspondence should be addressed: 3320B MSRB III, 1150 W. Medical Center Dr., University of Michigan, Ann Arbor, MI 48109-0600. Tel.: 734-615-5238; E-mail: rbanerje@umich.edu.
[2] The abbreviations used are: CBS, cystathionine β-synthase; PLP, pyridoxal 5′-phosphate; AdoMet, *S*-adenosylmethionine.

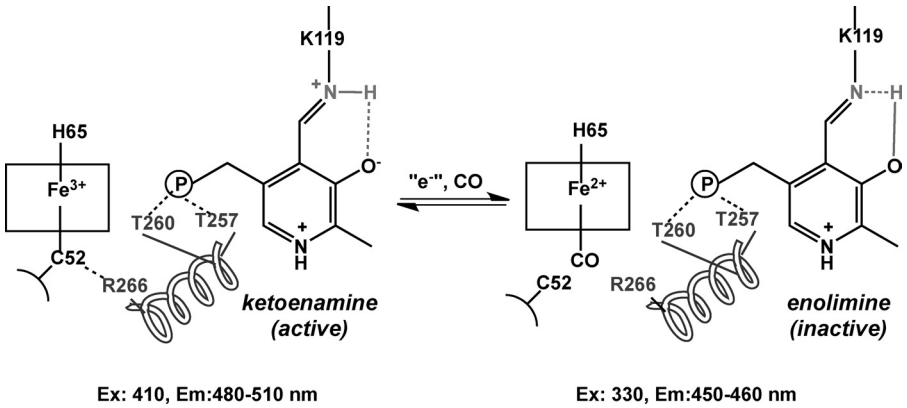

SCHEME 1. **PLP tautomers in CBS**.

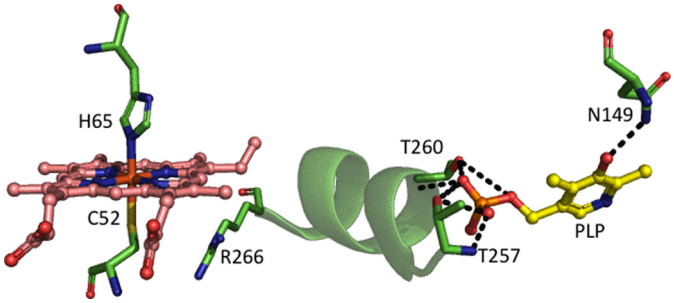

FIGURE 1. **Close-up of the heme and PLP pockets in human CBS.** The heme ligand residues and other select residues on α-helix 8 that might be important for communication between the heme and PLP sites are shown. This figure was generated using Protein Data Bank file 1M54.

inhibition. The structure of human CBS (10, 12) reveals that α-helix 8 extends between the heme and PLP pockets (Fig. 1) and suggests it as a candidate structural element important for signal transduction between the two cofactors (20). At one end of the helix, the side chain of Arg-266 is involved in an electrostatic interaction with the thiolate of Cys-52, which is a heme ligand (Fig. 1). The other end of α-helix 8 leads into the phosphate-binding loop, and multiple hydrogen-bonding interactions extend between Gly-256, Thr-257, Gly-258, Gly-259, and Thr-260 and the phosphate moiety of PLP.

PLP exists in tautomeric equilibrium between the inactive enolimine and the active ketoenamine forms (7, 15, 21, 22), which can be distinguished by fluorescence (Scheme 1) and resonance Raman spectroscopies (23). A hydrogen bond between the phenolic oxygen of PLP and Asn-149 in the active site stabilizes the ketoenamine tautomer (Fig. 1). Changes in the heme environment (*e.g.* formation of ferrous-CO CBS) result in a shift in the equilibrium to the enolimine form (23). This mechanism is supported by the behavior of the ferrous R266M CBS, in which the mutation disrupts the electrostatic interaction with Cys-52 and favors formation of a 424 nm-absorbing heme species, referred to as C424, which is inactive (24). Spectroscopic characterization of the inactive R266M mutant revealed that it is in the enolimine state (23).

In this study, we have examined whether perturbations at the PLP end of α-helix 8 are communicated to the heme site and characterized their effects on CBS activity. To this end, mutations at Thr-257 and Thr-260, which interact with the phosphate group of PLP, were introduced into recombinant human CBS to assess the effects of changes in polarity (Thr → Val), flexibility (Thr → Ser), and size (Thr → Ile/Met). Of these, T257M has been described in a homozygous form in an Italian homocystinuric patient, who is nonresponsive to pyridoxine supplementation (25). Our study provides the first evidence for perturbations in the PLP site being communicated to the heme site and establishes the importance of a helical secondary structure element in CBS for bidirectional communication between the cofactors and for stabilization of active PLP tautomer.

EXPERIMENTAL PROCEDURES

Materials—[^{14}C]Serine (164 mCi/mmol) was purchased from PerkinElmer Life Sciences. All other chemicals were purchased from Sigma or Fisher.

Construction of CBS Mutants—The CBS mutants were generated using wild-type CBS cloned in the pGEX4T1 plasmid in which the CBS cDNA is fused in frame with glutathione *S*-transferase (GST) (26). The following set of forward primers in which the mutagenic codon is underlined, were used to introduce missense mutations: T257M, 5′-TTCAGTGGGCATGGGCGGCACCATCACG-3′; T257I, 5′-TTCAGTGGGCATCGGCGGCACCATCACG-3′; T257S, 5′-TTCAGTGGGCTCCGGCGGCACCATCACG-3′; T257V, 5′-TTCAGTGGGCGTCGGCGGCACCATCACGG-3′; T260M, 5′-CACGGGCGGCATGATCACGGGCATTGC-3′; T260I, 5′-CACGGGCGGCATCATCACGGGCATTG-3′; T260S, 5′-CACGGGCGGCTCCATCACGGGCATTG-3′; T260V, 5′-CACGGGCGGCGTCATCACGGGCATTG-3′.

The reverse primers were complementary to the respective forward primers. The mutations were verified by nucleotide sequence analysis (Sequencing Core Facility, University of Michigan).

Expression and Purification of CBS Mutants—The recombinant wild-type and mutant CBSs were expressed and purified as described previously (27). Briefly, the cell pellet from a 6-liter culture was resuspended in 300 ml of 1× phosphate-buffered saline (PBS) containing a single protease inhibitor mixture tablet (Roche Applied Science) and 75 mg of lysozyme and stirred for 1.5 h at 4 °C. The cells were lysed by sonication, and the supernatant was obtained by centrifugation at 12,000 × *g* for 25 min. The supernatant was loaded onto a glutathione-Sepharose column pre-equilibrated with 1× PBS. The column was washed with 1× PBS, and GST-fused CBS was eluted with 50 mM Tris,

pH 8.0, containing 10 mM glutathione. This step was followed by thrombin digestion at 4 °C to remove the GST tag, following which the protein was loaded onto a Q Sepharose column (2.5 × 12 cm) equilibrated with 50 mM Tris buffer, pH 8.0, and then washed with same buffer. The protein was eluted with a 500-ml gradient ranging from 0 to 500 mM NaCl in 50 mM Tris-HCl, pH 8.0. The fractions of interest were concentrated and stored at −80 °C.

Estimation of PLP Content—The PLP content of CBS was determined by fluorescence spectroscopy as described previously (14). Fluorescence emission of the PLP oxime was detected at 446 nm following excitation at 353 nm. A standard curve was generated using PLP samples of known concentrations, which had been determined spectrophotometrically using $\epsilon_{295} = 5.1\ mM^{-1}\ cm^{-1}$ in 0.1 N HCl.

Enzyme Assay—Enzyme activity was measured using homocysteine and [^{14}C]serine as described previously (27). Briefly, a 200-μl assay mixture contained 250 mM Tris, pH 8.6, 0.5 mg/ml bovine serum albumin, 30 mM [^{14}C]serine (~40,000 dpm), 20 mM L-homocysteine. The reaction mixture was incubated at 37 °C for 5 min, and the reaction was started by the addition of 5.0 μg of purified CBS. The reaction was terminated after 30 min by the addition of 200 μl of 10% trifluoroacetic acid. In experiments testing the effect of AdoMet and PLP, 500 μM AdoMet and 250 μM PLP (final concentrations) were added to the reaction mixture during the preincubation. Formation of radiolabeled cystathionine was determined as described previously (27). The detection limit of this assay is ~0.4 μmol/h/ mg of protein.

Detection of H_2S—H_2S generation from cysteine plus homocysteine was measured using the lead sulfide assay as described previously (28) with the following modifications. The reaction mixture containing 250 mM Hepes buffer, pH 8.6, 0.4 mM lead acetate, 25 mM homocysteine, and CBS was preincubated at 37 °C for 4 min. The reaction was initiated by the addition of 25 mM cysteine. For experiments testing the effect of AdoMet, 500 μM AdoMet (final concentration) was added into the reaction mixture together with cysteine. For experiments testing the effect of PLP, 250 μM PLP (final concentration) was added to the reaction mixture during preincubation. An extinction coefficient of $5500\ M^{-1}\ cm^{-1}$ was used for estimation of lead sulfide concentration. The detection limit of this assay is ~10 μmol/ h/mg of protein.

Reduction, Carbonylation, and Reoxidation of CBS—CBS assays were conducted in an anaerobic chamber (with <0.3 ppm oxygen; Vacuum Atmospheres Co., Hawthorne, CA). The assays were performed with oxidized, reduced, and CO-bound CBS (5.0 μg) in 250 mM Tris buffer, pH 8.6, as described previously (15). Reactions were quenched with 10% trifluoroacetic acid after 30 min, and then samples were brought outside the chamber and processed as described previously (15). The CO-bound CBS samples were reoxidized by exposing them to air, pipetting up and down 3–4 times, and incubating overnight at 4 °C. To reduce CBS, sodium dithionite solution was added to a final concentration of 7 mM inside the anaerobic chamber. Ferrous-CO CBS was generated by purging the ferrous CBS sample in a tightly sealed quartz cuvette with CO for 10–15 min. Protein aliquots were removed, and enzyme activity was measured in the different redox and CO-bound states of CBS.

Analysis of PLP Tautomers by Fluorescence Spectroscopy—Unbound PLP was removed by concentrating the protein in a 30-kDa molecular weight cut-off Centricon filter at 4 °C until the volume was reduced by 80–90%. Fresh 100 mM sodium phosphate buffer, pH 8.0, was added to the sample in the Centricon concentrator, and this process was repeated four times. Fluorescence emission spectra of each CBS sample (40 μM) in the ferric, ferrous, heat-inactivated ferrous, and CO-bound states (maintained under a nitrogen atmosphere) were recorded in 100 mM sodium phosphate buffer (pH 8.0) in sealed quartz fluorescence cells as described earlier (23). Fluorescence spectra were measured using excitation wavelengths of 330 and 410 nm. For 330 nm excitation, the emission spectrum was recorded using an excitation slit width of 10 nm, emission slit width of 10 nm, and scan rate of 25 nm/min. For 410 nm excitation, the emission spectrum was recorded using an excitation slit width of 10 nm, emission slit width of 20 nm, and scan rate of 100 nm/min.

RESULTS

PLP Content and Activities of Ferric CBS Mutants—The yields of purified T257I, T257V, T260M, T260S, and T260V proteins (~7.0 mg/liter of culture) were similar to that of wild-type CBS. In contrast, the yield of T257S was ~3-fold higher (~21.0 mg/liter of culture) than that of wild-type CBS, whereas the yield of T257M CBS was lower (~1.0 mg/liter of culture). The T260I protein was obtained in extremely low yield and was very susceptible to degradation during the purification process, which precluded its further characterization. The purity of each mutant protein was judged to be >90% by SDS-PAGE analysis. The PLP contents of T257S (1.1 ± 0.04/mol of active site) T260M (0.7 ± 0.1), T260S (1.2 ± 0.1) and T260V CBS (0.85 ± 0.05) were similar to that of wild-type enzyme (1.2 ± 0.1), whereas contents of T257M (0.37 ± 0.14), T257I (0.37 ± 0.05), and T257V (0.51 ± 0.05) CBS were lower (Table 1). The activities of the mutant enzymes were assessed under aerobic conditions and in the presence or absence of exogenous PLP in the standard radioactive assay (Table 2). The basal activities of the mutants were ~4-fold (T257S CBS), ~5-fold (T260V CBS), ~7-fold (T260M CBS), 17-fold (T257M and T257V CBS), and ~100-fold (T257I CBS) lower than for wild-type enzyme, whereas the activity of T260S CBS was similar to that of wild-type CBS. The specific activities of the mutant proteins do not correlate with their PLP content (Table 1). The addition of PLP to the assay mixture did not elicit a significant change in the activities of most mutant enzymes with the exception of the T257I mutant, which was activated ~3-fold upon PLP addition. The insensitivity of the patient T257M mutation to PLP predicts a pyridoxine-nonresponsive phenotype. Wild-type CBS and T260S CBS were activated ~2-fold in the presence of AdoMet (29). The other mutants examined in this study showed markedly different responses, varying from 2-fold inhibition by AdoMet (for T257M and T257I) to ~3-fold activation (for T257S and T260V) and ~6-fold activation (for T260M) by AdoMet. In contrast, the presence of PLP + AdoMet resulted

TABLE 1
Kinetic parameters for wild-type *versus* mutant CBSs

CBS	Specific activity				PLP content
	−PLP, −AdoMet	+PLP	+AdoMet	+PLP, +AdoMet	
	μmol/h/mg protein				*mol PLP/mol subunit*
Wild type	215 ± 19	227 ± 29	490 ± 15	499 ± 13	1.2 ± 0.1
T257M	12 ± 2	11 ± 2	2 ± 1	5 ± 1	0.37 ± 0.14
T257I	2 ± 1	7 ± 1	1 ± 0.5	3 ± 1	0.37 ± 0.05
T257S	56 ± 10	82 ± 16	166 ± 20	310 ± 40	1.1 ± 0.05
T257V	15 ± 5	18 ± 6	17 ± 4	38 ± 10	0.51 ± 0.05
T260M	30 ± 10	33 ± 10	168 ± 18	176 ± 11	0.7 ± 0.1
T260S	268 ± 47	300 ± 39	532 ± 9	720 ± 62	1.2 ± 0.1
T260V	77 ± 8	97 ± 5	220 ± 40	483 ± 62	0.85 ± 0.05

TABLE 2
H_2S generation by wild-type and mutant CBSs

CBS	Specific activity			
	−PLP, −AdoMet	+PLP	+AdoMet	+PLP, +AdoMet
	μmol/h/mg protein			
Wild type	330 ± 48	366 ± 60	1140 ± 156	1263 ± 186
T257M	ND[a]	ND	ND	ND
T257I	30 ± 6	120 ± 24	18 ± 6	108 ± 24
T257S	144 ± 12	222 ± 30	612 ± 60	894 ± 72
T257V	210 ± 24	336 ± 36	444 ± 114	534 ± 36
T260M	12 ± 1	24 ± 2	72 ± 6	108 ± 6
T260S	396 ± 72	402 ± 60	1470 ± 198	1446 ± 276
T260V	54 ± 18	72 ± 24	270 ± 42	342 ± 78

[a] ND, not detectable.

in an additional ~1.3-fold (T257S) and ~2-fold (T260S, T257V, and T260V) activation (Table 1).

H_2S Biogenesis by CBS Mutants—The specific activities of the mutants for H_2S production were differentially impacted compared with the effects in the canonical transsulfuration reaction (Table 2). Thus, H_2S production was either comparable (T260S) or ~2-fold (T257S CBS and T260V CBS), ~6-fold (T260V CBS), 11-fold (T257I CBS), or ~27-fold (T260V CBS) lower than for wild-type CBS. The addition of PLP to the assay mixture elevated the specific activity of T257I CBS (~4-fold) and T260V CBS (~2 fold) but did not have a significant effect on the activities of the other mutants. The addition of exogenous AdoMet to the reaction mixture increased the activities of wild-type and T260S CBS ~3.5-fold, whereas the other mutants showed an ~2-fold (T257V CBS), 4-fold (T257S CBS), or ~5-fold (T260V CBS) activation. In contrast, T257I CBS showed an ~2-fold inhibition in the presence of AdoMet. The addition of PLP and AdoMet enhanced the activity only slightly compared with AdoMet for all mutants. The only exception was the T257M mutant, in which activity was not detectable in the presence or absence of PLP and AdoMet (Table 2).

Effect of Carbonylation and Reoxidation on Activity of Ferrous CBS Mutants—The UV-visible spectrum of each mutant in the ferric state was identical to that of wild-type CBS and exhibited a Soret maximum at 428 nm and a broad α,β band centered at ~550 nm (Fig. 2). For wild-type CBS (Fig. 2*A*) and the T260S mutant (Fig. 2*G*), the ferrous Soret peak shifted to 449 nm, and the α,β bands sharpened at 540 and 570 nm, respectively. In contrast, the T257M and T257I CBS converted to a state previously described as C424 CBS (24), based on the position of the Soret maximum at 424 nm (Fig. 2, *B* and *C*). Although the spectra of the ferrous T257S, T257V, T260M, and T260V mutants were similar to that of wild-type CBS (Fig. 2, *D*, *E*, *F*, and *H*), the 424 nm shoulder associated with inactive enzyme (30, 31) was more prominent.

The activities of the CBS mutants were further characterized in the ferrous and ferrous-CO states and compared with that of wild-type CBS (Table 3). The specific activities of the wild-type and mutant ferric CBSs assayed under anaerobic conditions were comparable with their activities monitored under aerobic conditions (Table 1). The specific activities of wild-type, T257S, T260S, and T260V ferrous CBSs were ~2-fold lower than in the ferric state. In contrast, the activities of the other mutants in the ferrous state were severely affected. Indeed, the activity of ferrous T257M was undetectable due to formation of the inactive C424 species exclusively upon reduction (Fig. 2*B*). The activity of ferrous T260M CBS diminished 6-fold, whereas the activities of ferrous T257I and T257V were suppressed 8–10-fold in comparison with the ferric state, consistent with a higher proportion of these enzymes converting to the C424 species (Fig. 2, *C*, *E*, and *F*).

Formation of the ferrous CBS-CO species resulted in the expected shift in the Soret peak from 449 to 420 nm for wild-type CBS and the mutants (Fig. 2). Carbonylation of wild-type CBS resulted in ~90% loss of activity compared with the ferric enzyme, as seen previously (15). In contrast, T260S CBS lost 97% of its activity, and the activities of the ferrous-CO forms of the other mutants were not detectable. Carbonylation of wild-type CBS was reversed by air oxidation as evidenced by the reappearance of the ferric Soret peak at 428 nm (Fig. 2*A*) and almost complete recovery of enzyme activity (Table 3). In contrast, the Soret peaks of reoxidized T257M, T257I, and T257V remained at 420 nm with loss of peak intensity (Fig. 2, *B*, *C*, and *E*), and the Soret peaks of reoxidized T257S, T260M, T260S, and T260V CBS were slightly blue-shifted to 425–426 nm (Fig. 2, *D*, *F*, *G*, and *H*). Reoxidation was associated with recovery of ~90, 40, 20, 15, and 5% of CBS activity, respectively, for wild-type, T257S, T260S, T260V, and T260M CBS, respectively, whereas the activity of the remaining mutants was undetectable upon reoxidation (Table 3). These results indicate that mutations at the Thr-257 and Thr-260 residues in the PLP binding pocket perturb the heme electronic environment and lead to trapping of the enzyme in an inactive form following formation of the ferrous-CO complex.

Analysis of PLP Tautomers by Fluorescence Spectroscopy—Fluorescence spectroscopy was used to assess the effect of mutations at the Thr-257 and Thr-260 positions on the PLP tautomeric equilibrium (Figs. 3–6). The ketoenamine and enolimine tautomers exhibit broad emission bands with maxima at

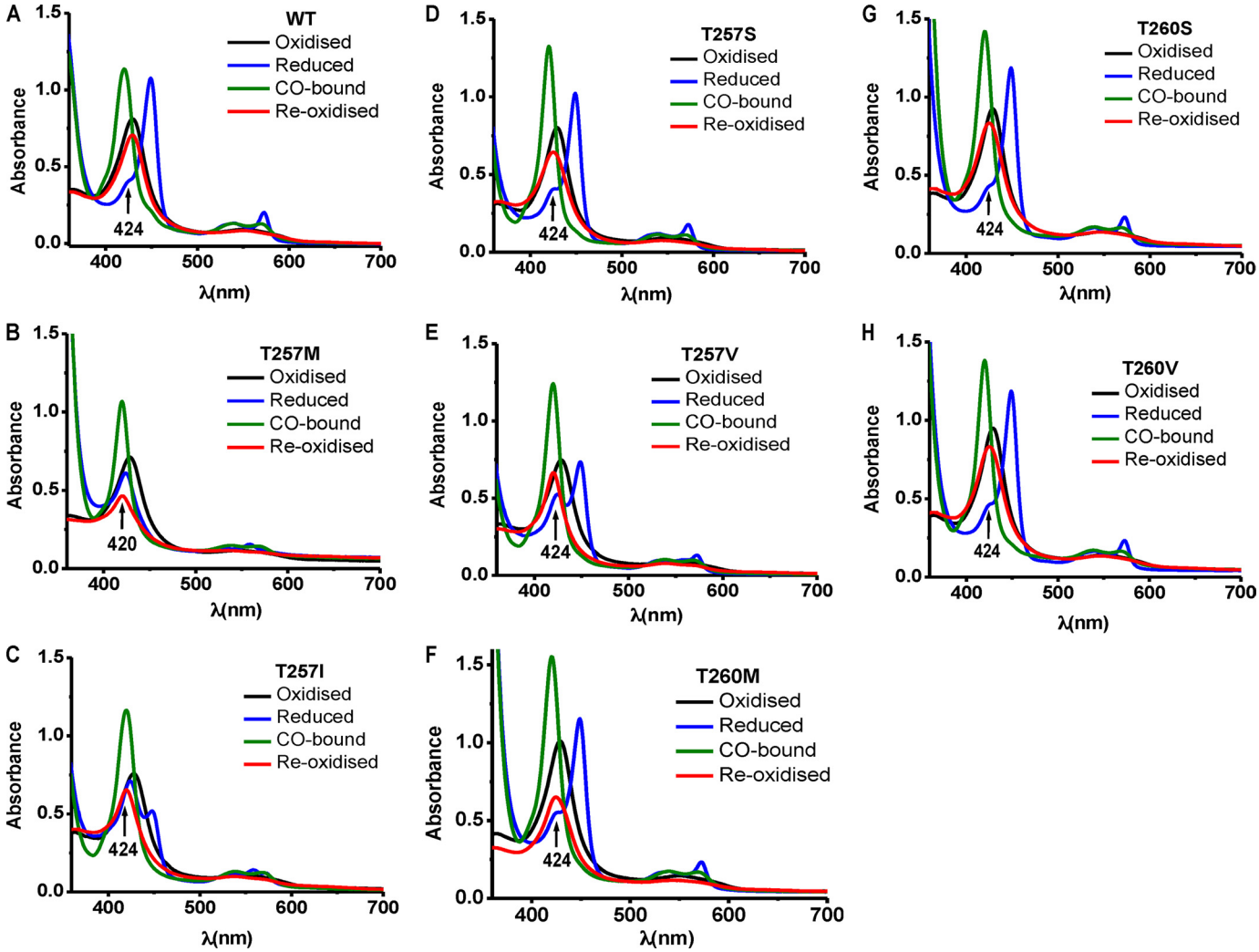

FIGURE 2. **UV-visible spectra of CBS.** The spectra were recorded in 50 mM Tris buffer, pH 8.6, at room temperature using 8 μM wild-type CBS (*A*), 8 μM T257M (*B*), and 10 μM T257IM (*C*), T257S (*D*), T257V (*E*), T260M (*F*), T260S (*G*), and T260V (*H*) inside an anaerobic glove box. Wild-type ferric CBS exhibits a Soret peak at 428 nm (*black*), which shifts to 449 nm (*blue*) upon reduction with dithionite. The ferrous-CO species has a Soret maximum at 420 nm (*olive*), which returns to 428 nm (*red*) upon overnight air oxidation of wild-type, to 425 nm with T257S, T260M, and T260V, or to 426 nm with T260S CBS and remains at 420 nm with T257I, T257M, and T257V.

TABLE 3
Effect of heme reduction and carbonylation on CBS activity

CBS	Specific activity (+PLP, +AdoMet)			
	Ferric	Ferrous	Ferrous-CO	Reoxidized[a]
	μmol/h/mg protein			
Wild type	491 ± 9	241 ± 34	51 ± 5	457 ± 16
T257M	5 ± 1	ND[b]	ND	ND
T257I	3 ± 0.5	0.4 ± 0.2	ND	ND
T257S	300 ± 40	166 ± 12	ND	124 ± 14
T257V	39 ± 6	4 ± 1	ND	ND
T260M	168 ± 12	28 ± 8	ND	9 ± 1
T260S	580 ± 60	284 ± 10	21 ± 2	116 ± 16
T260V	264 ± 35	130 ± 16	ND	40 ± 12

[a] Ferrous-CO samples that were air-oxidized.
[b] ND, not detectable.

480–510 nm and ~450–460 nm (32, 33), respectively (Scheme 1). The emission maximum of the enolimine tautomer associated with wild-type ferrous-CO CBS is between 450 and 460 nm (Fig. 3*A*, 330 nm excitation, *green spectrum*), whereas the emission maximum of the ketoenamine form associated with ferric and ferrous CBS lies between 480 and 510 nm (Fig. 4*A*, 410 nm excitation, *black* and *blue spectra*) (23).

The emission spectrum of ferric T257M CBS showed a broad peak centered at ~500 nm (Fig. 3*B*) and at 490 nm (Fig. 4*B*) upon excitation at 330 and 410 nm, respectively. Upon reduction with sodium dithionite, the heme in T257M CBS is fully converted to the C424 species (Fig. 2*B*). However, the fluorescence changes accompanying reduction of the T257M mutant were distinct from those seen for the C424 species formed with wild-type CBS. Reduction of T257M CBS resulted in a large decrease in the ~500 nm emission peak intensity, and the new peak was centered at 481 nm (Fig. 3*B*). In contrast, formation of wild-type C424 CBS resulted in a shift in the peak from 506 nm (ferric CBS) to 483 nm (ferrous CBS) to 464 nm (C424 CBS) (Fig. 3*A*). With 410 nm excitation, a significant increase in intensity and a shift in the peak position from 505 nm (ferric) to 496 nm (ferrous) to a double-humped feature with peaks at 483 and 462 nm (C424 CBS) were observed (Fig. 4*A*). In contrast, the T257M mutant showed a very slight peak shift toward lower wavelength without a significant change in the peak intensity in going from the ferric to ferrous state (Fig. 4*B*). The addition of CO to the C424 T257M mutant resulted in formation of the

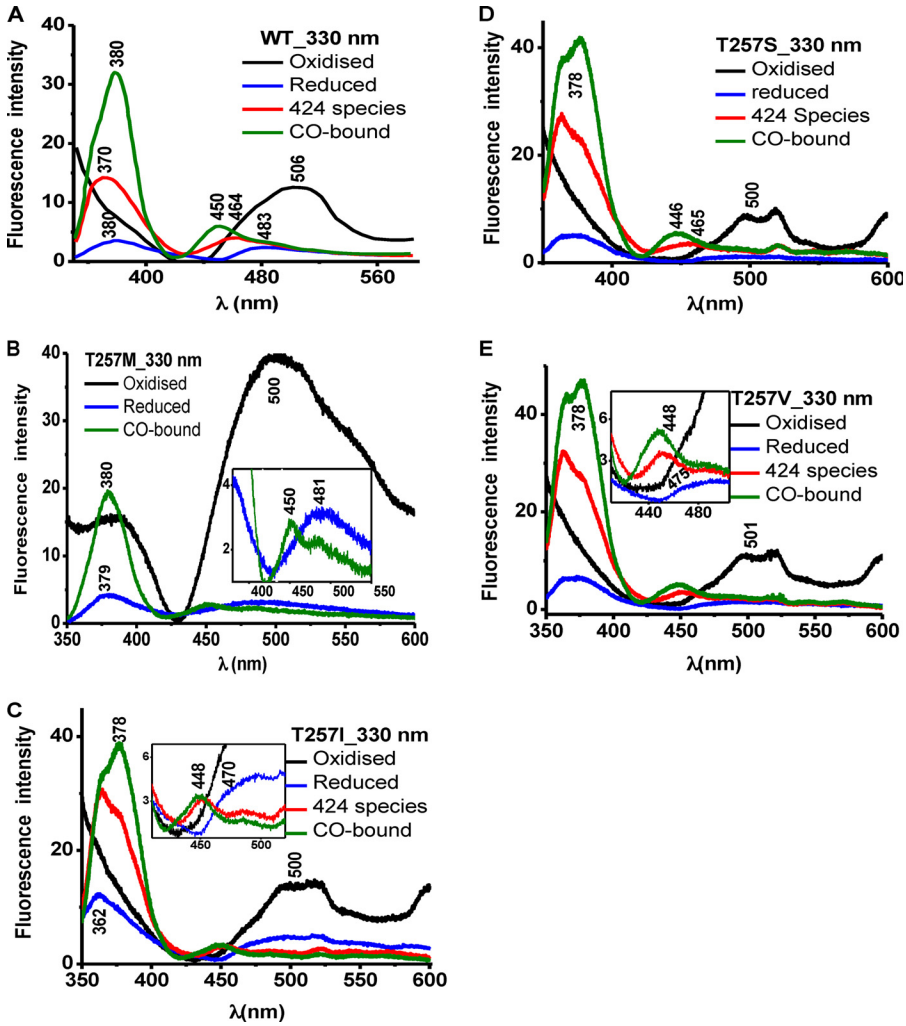

FIGURE 3. **Comparison of PLP tautomeric forms of wild-type CBS and Thr-257 mutants.** Fluorescence emission spectra of 40 μM wild-type CBS (*A*) in 100 mM phosphate buffer, pH 8.0, and of the T257M (*B*), T257I (*C*), T257S (*D*), and T257V (*E*) CBS mutants. The excitation wavelength was 330 nm.

ferrous-CO adduct as evidenced by a shift in the Soret maximum to 420 nm (Fig. 2*B*). The fluorescence spectrum of this adduct exhibited a maximum at ~450 nm with a shoulder at ~467 nm with 330 nm excitation (Fig. 3*B*, *inset*) and a maximum at ~484 nm with a shoulder at ~454 nm with 410 nm excitation (Fig. 4*B*). The appearance of fluorescence emission in the 450–460 nm region is consistent with a shift in the tautomeric equilibrium toward the inactive enolimine species, and such shifts were also seen for wild-type CBS, although with a significantly greater peak intensity.

The fluorescence spectrum of ferric T257I CBS showed an emission peak centered at ~500 nm after excitation with either 330 or 410 nm (Figs. 3*C* and 4*C*, *black*). The spectrum of ferrous T257I CBS obtained with 330 nm excitation showed a peak at ~490 nm with a shoulder at ~470 nm (Fig. 3*C*, *inset*, *blue*) and a peak at ~490 nm with 410 nm excitation (Fig. 4*C*, *blue*). Complete conversion of ferrous T257I CBS to the 424 species by heating at 55 °C for 15 min, as described previously (34), shifted the emission peak to ~448 nm (Fig. 3*C*, *inset*, *red*) or to ~452 with a shoulder at ~482 nm (Fig. 4*C*, *red*). Carbonylation of the C424 species resulted in emission peaks at ~448 and ~444 nm (Figs. 3*C* and 4*C*, *green*). The fluorescence spectra of the T257S and T257V mutants were qualitatively similar to those of T257I CBS (Figs. 3 (*D* and *E*) and 4 (*D* and *E*)).

The fluorescence spectra of ferric T260M CBS showed emission peaks centered at ~500 nm with either 330 or 410 nm excitation (Figs. 5*B* and 6*B*, *black*). Reduction and excitation of the resulting ferrous protein produced an emission maximum at ~490 nm and significant loss in peak intensity with 330 nm (Fig. 5*B*, *blue*). Excitation at 410 nm resulted in only a slight loss in peak intensity (Fig. 6*B*, *blue*) unlike wild-type CBS, which showed a more significant change (Fig. 6*A*). The fluorescence spectra of the C424 species generated by heating exhibited maxima at ~468 nm (330 nm excitation) or at ~475 nm with a significant loss of intensity (410 nm excitation) (Figs. 5*B* and 6*B*, *red*). The fluorescence spectra of the ferrous-CO form of T260M CBS exhibited emission maxima at ~468 nm with a shoulder at ~452 nm (Fig. 5*B*, *green*) and at ~458 nm (Fig. 6*B*, *green*). The spectra of the C424 and ferrous-CO forms of T260M CBS are consistent with a tautomeric shift to the enolimine species.

The fluorescence spectra of the T260S and T260V mutants were qualitatively similar to those of wild-type CBS (Figs. 5 (*C* and *D*) and 6 (*C* and *D*)).

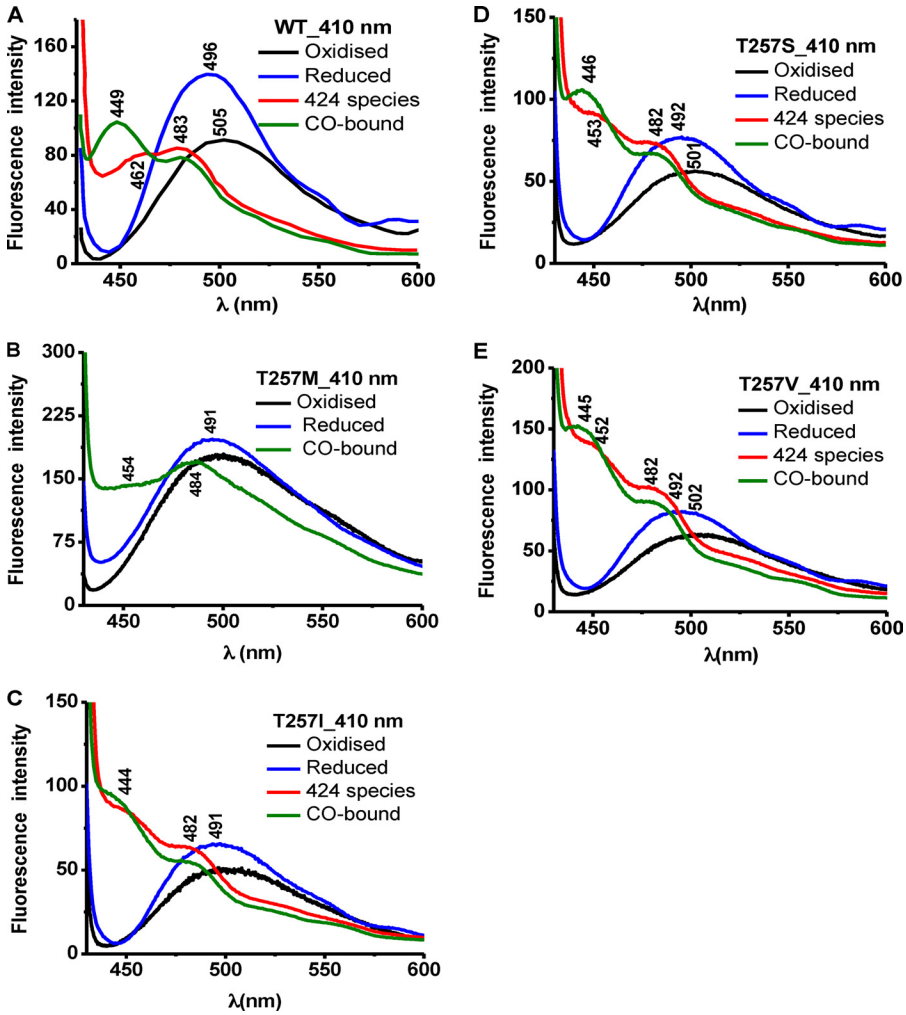

FIGURE 4. **Comparison of PLP tautomeric forms of wild-type CBS and Thr-257 mutants.** Fluorescence emission spectra of 40 μM wild-type CBS (*A*) in 100 mM phosphate buffer, pH 8.0, and of the T257M (*B*), T257I (*C*), T257S (*D*), and T257V (*E*) CBS mutants. The excitation wavelength was 410 nm.

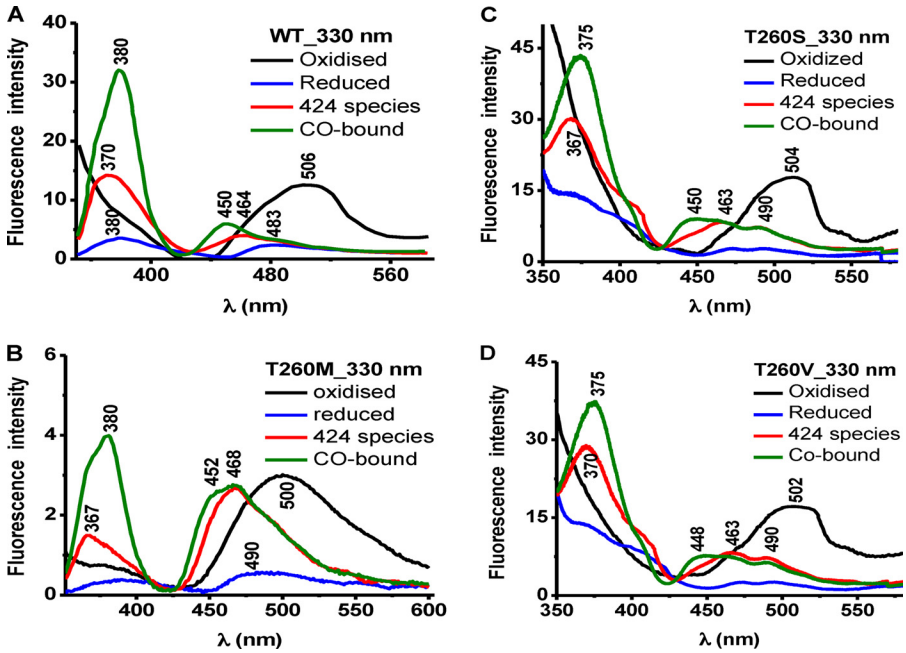

FIGURE 5. **Comparison of PLP tautomeric forms of wild-type CBS and Thr-260 mutants.** The fluorescence emission spectra are shown for 40 μM wild-type CBS (*A*) in 100 mM phosphate buffer, pH 8.0, and of the T260M (*B*), T260S (*C*), and T260V (*D*) CBS mutants. The excitation wavelength was 330 nm.

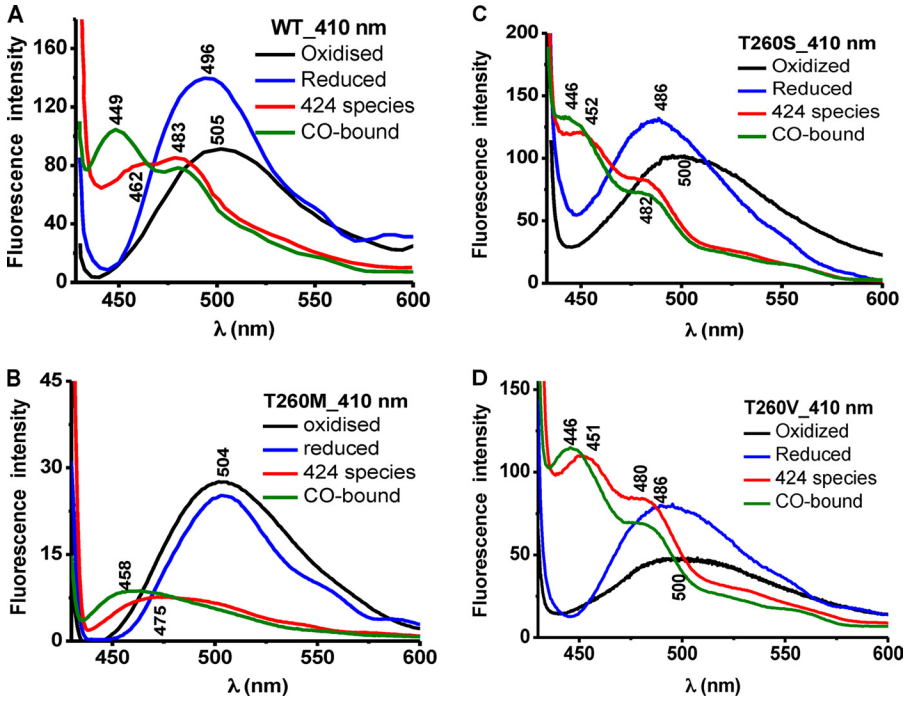

FIGURE 6. **Comparison of PLP tautomeric forms of wild-type CBS and Thr-260 mutants.** The fluorescence emission spectra are shown for 40 μM wild-type CBS (*A*) in 100 mM phosphate buffer, pH 8.0, and of the T260M (*B*), T260S (*C*), and T260V (*D*) CBS mutants. The excitation wavelength was 410 nm.

DISCUSSION

In this study, we have investigated the hypothesis that bidirectional communication between the distant PLP- and heme-binding sites is exerted via α-helix 8 in human CBS. Specifically, we have investigated the roles of two residues, Thr-257 and Thr-260, which reside on a loop leading into the PLP-end of α-helix 8 (Fig. 1). The side chains and backbone of Thr-257 and Thr-260 are engaged in hydrogen-bonding interactions with the oxygen atoms on the phosphate group of PLP. The threonine residues are conserved in CBS sequences and, in fact, are also seen in other PLP-dependent enzymes (12). Each of these threonine residues was mutated to methionine, isoleucine, serine, and valine, respectively, although the insolubility of the T260I mutant precluded its characterization. T257M mimics a patient mutation (25).

In general, mutations at the Thr-257 position affected enzyme activity more adversely than at the Thr-260 position in the following order of substitutions: Ile < Met < Val < Ser. Because the Thr → Ser substitution is the most conservative, it is not surprising that T257S was less severely affected than substitutions by other residues at this position. In fact, the Thr → Ser substitution at position Thr-260 yielded a more robust enzyme.

Six of the seven mutants exhibit lower activity than wild-type enzyme (ranging from ~2- to ~500-fold, respectively, in the presence of AdoMet). Because diminution in enzyme activity was greater than the decrease in their PLP content, which ranged from 30 to 100% of wild-type CBS, it suggests that the impairments caused by the mutations are not simply due to changes in cofactor occupancy. The activity of the T260S mutant was 1.3- and 1.4-fold higher in the absence and presence of AdoMet + PLP, respectively. AdoMet elicited unexpected effects on some of the other CBS mutants. Thus, the T257S, T260M, and T260V CBSs were hyperactivated (~6-fold) compared with wild-type enzyme, whereas the T257M and T257I mutants were inhibited ~2-fold (Table 1). The T257V and T260S CBSs are activated ~2–3-fold by AdoMet as reported previously for wild-type enzyme (29). These results identify residues around the phosphate group of PLP as being sensitive to allosteric activation by the regulatory domain of CBS, where AdoMet binds (35). The pathogenic T257M mutation exhibited both very low intrinsic activity and inhibition by AdoMet, and its activity was unresponsive to PLP.

Interestingly, mutations at the 257 *versus* 260 position elicited contrasting effects on H_2S production (Table 2). In general, mutations at the 257 position impacted H_2S elimination in the cysteine + homocysteine assay more adversely than H_2O elimination in the standard serine + homocysteine assay (compare Tables 1 and 2). Hence, T257I and T257V showed lower activity in the canonical (<1 and 2.5%) *versus* H_2S (~9 and 43%) assays as compared with wild-type CBS. In contrast, the T260M and T260V mutants exhibited higher activity in the canonical (35 and 97%) *versus* H_2S-generating (~9 and 28%) assays as compared with wild-type CBS. The conservative Thr → Ser substitutions at both positions had the mildest phenotype, and the specific activity of the T260S mutant for H_2S generation was higher than that of the wild-type enzyme.

With the exception of T257S mutation, the other substitutions at this position led to very significant loss of activity in the ferrous state (Table 3). This can be explained by the greater susceptibility of these mutants to form the inactive C424 species upon reduction (Fig. 2, *B–E*). Wild-type ferrous CBS converts to the C424 species at elevated temperatures and/or pH 7 (30, 34). The identity of the heme ligand that replaces the thio-

late of Cys-52 in the C424 species is not known and, based on spectroscopic studies, is expected to be a neutral ligand (*e.g.* water, a protonated thiol, an imidazole side chain, or a backbone amide oxygen) (24). With the exception of the T260M mutant, which showed ~6-fold lower activity in the ferrous state, the other two Thr-260 mutants exhibited ~2-fold lower activity like wild-type CBS.

Binding of CO to ferrous CBS inhibits CBS activity, communicated allosterically via α-helix 8 (17). As with wild-type enzyme (Fig. 2*A*), binding of CO to the mutant enzymes in the ferrous state shifted the Soret maximum to 420 nm (Fig. 2, *B–H*). Whereas the activity of wild-type and T260S CBSs was inhibited ~90–96% in the ferrous-CO state, the activity of all other mutants was undetectable (Table 3). Air oxidation of wild-type CBS resulted in the return of spectral features characteristic of ferric CBS with a Soret maximum at 428 nm (Fig. 2*A*) and was accompanied by an almost quantitative recovery of activity (Table 3). In contrast, air oxidation of a subset of mutants resulted in significant loss of peak intensity and a slight blue shift in the Soret maximum to 425 nm (T257S, T260M, and T260V) (Fig. 2). Air oxidation of ferrous-CO T257M and T257M/I/V CBSs also resulted in a significant loss of the Soret peak intensity, which remained at 420 nm. To determine whether the loss in peak intensity was due to heme dissociation from the protein, a couple of the air-oxidized CBS mutants were concentrated using a Centricon filter with a 10 kDa cutoff. The spectrum of the filtrate showed loss of heme from the air-oxidized T257M and T260M samples (not shown). In contrast, the corresponding filtrate obtained from air-oxidized wild-type enzyme was devoid of absorption. Consistent with the spectral data, very low recovery of enzyme activity was obtained after air oxidation for most of the mutants that showed a loss in the heme absorption spectrum.

The evidence for heme-based allosteric regulation of human CBS derives from the demonstration that reductive nitrosylation or carbonylation results in inhibition of enzyme activity (16, 18). In our model of allosteric communication between the heme and PLP sites, displacement of the Cys-52 ligand by CO (or NO) leads to loss of its hydrogen bonding interaction with Arg-266, which is communicated via α-helix 8 to the active site (17, 23, 24). Conversely, mutation of Arg-266 to methionine leads to rapid formation of the inactive C424 species upon reduction (24). In this study, we provide evidence, for the first time, for signal transduction in the opposite direction (*i.e.* from the PLP pocket to the heme). Thus, the T257M patient mutation elicits changes in the heme electronic environment, resulting in facile formation of the C424 species upon heme reduction (Fig. 2*B*) and, in this way, resembles the R266M mutation at the opposite end of α-helix 8. The remaining mutants are intermediate between wild-type and R257M CBS in their propensity for conversion to the inactive ferrous state, and a mixture of species with Soret maxima at 449 and 424 nm is formed upon reduction (Fig. 2, *C–H*). Formation of the C424 species in the T257M, but not as much in the other mutants, is associated with a significant shift in the PLP tautomeric equilibrium toward the ketoenamine species. These differences, together with changes in the relative intensities of the fluorescence emission spectra between the mutants and wild-type CBS, indicate that factors in addition to the inactive PLP tautomer and low PLP content combine to define their phenotypes.

Structural insights into how mutations of the two threonine residues in the PLP binding pocket are transmitted to the heme site would be useful. However, so far, the only available structures of human CBS are of the truncated catalytic core lacking the C-terminal regulatory domain (10, 12), However, the kinetic properties of the truncated human enzyme are significantly different from those of the full-length one in addition to the loss of AdoMet-dependent allosteric regulation. Recently, the structure of the full-length *Drosophila* CBS has been reported (11). However, unlike the human enzyme, AdoMet does not regulate *Drosophila* CBS, and its kinetic properties resemble those of the truncated rather than the full-length human enzyme. The fact that the threonine mutations alter AdoMet-dependent regulation suggests that these residues in the catalytic core are also important for transmission of allosteric communication from the regulatory AdoMet-binding domain.

In conclusion, our results support a model for transmission of allosteric communication in CBS between the heme cofactor and the PLP-containing active site via α-helix 8. The low PLP content of the T257M mutant, its insensitivity to exogenous PLP, and its very low activity under steady-state turnover conditions are consistent with the pathogenic and pyridoxine-nonresponsive phenotype of the homocystinuric patient in which this mutation has been described (25). Substitutions at both Thr-257 and Thr-260 positions affect the electronic environment of the heme, which is readily seen in the ferrous state by the enhanced propensity for formation of the inactive C424 species and the very poor recovery of activity upon air oxidation of the ferrous-CO form. These studies are consistent with the role of α-helix 8 not only in signal transduction between the cofactor binding sites but also for stabilizing an active conformation of CBS. Characterization of the seven mutations at the two threonines also reveals the different susceptibilities of the canonical condensation reaction between serine and homocysteine *versus* the H_2S-generating reaction between cysteine and homocysteine, suggesting the potential for independent regulation of these two activities. Finally, the altered sensitivity of the threonine mutants to AdoMet regulation suggests a role for these residues in signal transmission from the second allosteric effector, AdoMet, to the catalytic core of CBS.

REFERENCES

1. Banerjee, R., Evande, R., Kabil, O., Ojha, S., and Taoka, S. (2003) Reaction mechanism and regulation of cystathionine β-synthase. *Biochim. Biophys. Acta* **1647,** 30–35
2. Miles, E. W., and Kraus, J. P. (2004) Cystathionine β-Synthase. Structure, Function, Regulation, and Location of Homocystinuria-causing Mutations. *J. Biol. Chem.* **279,** 29871–29874
3. Singh, S., and Banerjee, R. (2011) PLP-dependent H_2S biogenesis. *Biochim. Biophys. Acta* **1814,** 1518–1527
4. Kabil, O., and Banerjee, R. (2010) Redox Biochemistry of Hydrogen Sulfide. *J. Biol. Chem.* **285,** 21903–21907
5. Kraus, J. P., Janosík, M., Kozich, V., Mandell, R., Shih, V., Sperandeo, M. P., Sebastio, G., de Franchis, R., Andria, G., Kluijtmans, L. A., Blom, H., Boers, G. H., Gordon, R. B., Kamoun, P., Tsai, M. Y., Kruger, W. D., Koch, H. G., Ohura, T., and Gaustadnes, M. (1999) Cystathionine β-synthase mutations in homocystinuria. *Hum. Mutat.* **13,** 362–375

6. Sen, S., and Banerjee, R. (2007) A pathogenic linked mutation in the catalytic core of human cystathionine β-synthase disrupts allosteric regulation and allows kinetic characterization of a full-length dimer. *Biochemistry* **46,** 4110–4116
7. Taoka, S., Widjaja, L., and Banerjee, R. (1999) Assignment of enzymatic functions to specific regions of the PLP-dependent heme protein cystathionine β-synthase. *Biochemistry* **38,** 13155–13161
8. Kery, V., Bukovska, G., and Kraus, J. P. (1994) Transsulfuration depends on heme in addition to pyridoxal 5′-phosphate. Cystathionine β-synthase is a heme protein. *J. Biol. Chem.* **269,** 25283–25288
9. Singh, S., Madzelan, P., and Banerjee, R. (2007) Properties of an unusual heme cofactor in PLP-dependent cystathionine β-synthase. *Nat. Prod. Rep.* **24,** 631–639
10. Meier, M., Janosik, M., Kery, V., Kraus, J. P., and Burkhard, P. (2001) Structure of human cystathionine β-synthase. A unique pyridoxal 5′-phosphate-dependent heme protein. *EMBO J.* **20,** 3910–3916
11. Koutmos, M., Kabil, O., Smith, J. L., and Banerjee, R. (2010) Structural basis for substrate activation and regulation by cystathionine β-synthase (CBS) domains in cystathionine β-synthase. *Proc. Natl. Acad. Sci. U.S.A.* **107,** 20958–20963
12. Taoka, S., Lepore, B. W., Kabil, O., Ojha, S., Ringe, D., and Banerjee, R. (2002) Human cystathionine beta-synthase is a heme sensor protein. Evidence that the redox sensor is heme and not the vicinal cysteines in the CXXC motif seen in the crystal structure of the truncated enzyme. *Biochemistry* **41,** 10454–10461
13. Ojha, S., Hwang, J., Kabil, O., Penner-Hahn, J. E., and Banerjee, R. (2000) Characterization of the heme in human cystathionine β-synthase by x-ray absorption and electron paramagnetic resonance spectroscopies. *Biochemistry* **39,** 10542–10547
14. Ojha, S., Wu, J., LoBrutto, R., and Banerjee, R. (2002) Effects of heme ligand mutations, including a pathogenic variant, H65R, on the properties of human cystathionine β-syntase. *Biochemistry* **41,** 4649–4654
15. Taoka, S., West, M., and Banerjee, R. (1999) Characterization of the heme and pyridoxal phosphate cofactors of human cystathionine β-synthase reveals nonequivalent active sites. *Biochemistry* **38,** 2738–2744
16. Taoka, S., and Banerjee, R. (2001) Characterization of NO binding to human cystathionine [beta]-synthase. Possible implications of the effects of CO and NO binding to the human enzyme. *J. Inorg. Biochem.* **87,** 245–251
17. Puranik, M., Nielsen, S. B., Youn, H., Hvitved, A. N., Bourassa, J. L., Case, M. A., Tengroth, C., Balakrishnan, G., Thorsteinsson, M. V., Groves, J. T., McLendon, G. L., Roberts, G. P., Olson, J. S., and Spiro, T. G. (2004) Dynamics of carbon monoxide binding to CooA. *J. Biol. Chem.* **279,** 21096–21108
18. Kabil, O., Weeks, C. L., Carballal, S., Gherasim, C., Alvarez, B., Spiro, T. G., and Banerjee, R. (2011) Reversible heme-dependent regulation of human cystathionine β-synthase by a flavoprotein oxidoreductase. *Biochemistry* **50,** 8261–8263
19. Green, E. L., Taoka, S., Banerjee, R., and Loehr, T. M. (2001) Resonance Raman characterization of the heme cofactor in cystathionine β-synthase. Identification of the Fe-S(Cys) vibration in the six-coordinate low spin heme. *Biochemistry* **40,** 459–463
20. Evande, R., Ojha, S., and Banerjee, R. (2004) Visualization of PLP-bound intermediates in hemeless variants of human cystathionine β-synthase. Evidence that lysine 119 is a general base. *Arch. Biochem. Biophys.* **427,** 188–196
21. Janosík, M., Oliveriusová, J., Janosíková, B., Sokolová, J., Kraus, E., Kraus, J. P., and Kozich, V. (2001) Impaired heme binding and aggregation of mutant cystathionine β-synthase subunits in homocystinuria. *Am. J. Hum. Genet.* **68,** 1506–1513
22. Kery, V., Poneleit, L., Meyer, J. D., Manning, M. C., and Kraus, J. P. (1999) Binding of pyridoxal 5′-phosphate to the heme protein human cystathionine β-synthase. *Biochemistry* **38,** 2716–2724
23. Weeks, C. L., Singh, S., Madzelan, P., Banerjee, R., and Spiro, T. G. (2009) Heme regulation of human cystathionine β-synthase activity. Insights from fluorescence and Raman spectroscopy. *J. Am. Chem. Soc.* **131,** 12809–12816
24. Singh, S., Madzelan, P., Stasser, J., Weeks, C. L., Becker, D., Spiro, T. G., Penner-Hahn, J., and Banerjee, R. (2009) Modulation of the heme electronic structure and cystathionine β-synthase activity by second coordination sphere ligands. The role of heme ligand switching in redox regulation. *J. Inorg. Biochem.* **103,** 689–697
25. Sebastio, G., Sperandeo, M. P., Panico, M., de Franchis, R., Kraus, J. P., and Andria, G. (1995) The molecular basis of homocystinuria due to cystathionine β-synthase deficiency in Italian families and report of four novel mutations. *Am. J. Hum. Genet.* **56,** 1324–1333
26. Shan, X., and Kruger, W. D. (1998) Correction of disease-causing CBS mutations in yeast. *Nat. Genet.* **19,** 91–93
27. Taoka, S., Ohja, S., Shan, X., Kruger, W. D., and Banerjee, R. (1998) Evidence for heme-mediated redox regulation of human cystathionine β-synthase activity. *J. Biol. Chem.* **273,** 25179–25184
28. Chiku, T., Padovani, D., Zhu, W., Singh, S., Vitvitsky, V., and Banerjee, R. (2009) H2S biogenesis by human cystathionine γ-lyase leads to the novel sulfur metabolites lanthionine and homolanthionine and is responsive to the grade of hyperhomocysteinemia. *J. Biol. Chem.* **284,** 11601–11612
29. Finkelstein, J. D., Kyle, W. E., Martin, J. L., and Pick, A. M. (1975) Activation of cystathionine synthase by adenosylmethionine and adenosylethionine. *Biochem. Biophys. Res. Commun.* **66,** 81–87
30. Pazicni, S., Lukat-Rodgers, G. S., Oliveriusová, J., Rees, K. A., Parks, R. B., Clark, R. W., Rodgers, K. R., Kraus, J. P., and Burstyn, J. N. (2004) The redox behavior of the heme in cystathionine β-synthase is sensitive to pH. *Biochemistry* **43,** 14684–14695
31. Cherney, M. M., Pazicni, S., Frank, N., Marvin, K. A., Kraus, J. P., and Burstyn, J. N. (2007) Ferrous human cystathionine β-synthase loses activity during enzyme assay due to a ligand switch process. *Biochemistry* **46,** 13199–13210
32. Strambini, G. B., Cioni, P., Peracchi, A., and Mozzarelli, A. (1992) Characterization of tryptophan and coenzyme luminescence in tryptophan synthase from *Salmonella typhimurium*. *Biochemistry* **31,** 7527–7534
33. McClure, G. D., Jr., and Cook, P. F. (1994) Product binding to the α-carboxyl subsite results in a conformational change at the active site of *O*-acetylserine sulfhydrylase-A. Evidence from fluorescence spectroscopy. *Biochemistry* **33,** 1674–1683
34. Pazicni, S., Cherney, M. M., Lukat-Rodgers, G. S., Oliveriusová, J., Rodgers, K. R., Kraus, J. P., and Burstyn, J. N. (2005) The heme of cystathionine β-synthase likely undergoes a thermally induced redox-mediated ligand switch. *Biochemistry* **44,** 16785–16795
35. Scott, J. W., Hawley, S. A., Green, K. A., Anis, M., Stewart, G., Scullion, G. A., Norman, D. G., and Hardie, D. G. (2004) CBS domains form energy-sensing modules whose binding of adenosine ligands is disrupted by disease mutations. *J. Clin. Invest.* **113,** 274–284